POTENTIAL OF WELL STIMULATION USING SMALL-DIAMETER LATERALS IN GEOTHERMAL RESERVOIRS

Elisabeth Peters[1], Cornelis R. Geel[1], Rohith Nair[1], Guido Blöcher[2]

[1] TNO, Utrecht, The Netherlands

[2] GFZ German Research Centre for Geosciences, Telegrafenberg, 14473 Potsdam, Germany

lies.peters@tno.nl

Keywords: radial jetting, well stimulation, uncertainty modelling

ABSTRACT

To economically develop a geothermal resource, wells with sufficient productivity are a key element. One of the options to enhance the productivity of a well are small-diameter laterals. With Radial Jet Drilling (RJD) laterals of up to 100 m in length can be jetted perpendicular from a well bore. This technique has been developed in the petroleum industry but is relatively new for geothermal applications and still under development. One of the limitations is that the jets cannot be steered and thus the realized path is uncertain. In this paper, we will analyse the potential benefits of stimulation with laterals created with RJD (also called radials). For two case studies, a sensitivity analysis was performed including the impact of the uncertainty in the lateral path and heterogeneity of the formation. The first case study is a layered reservoir with vertical wells. The second case study is a fractured reservoir in which the fracture distribution is determined by the distance to faults. The analysis showed in both reservoirs that the orientation of the radials with respect to the direction of highest permeability is an important factor for the performance of the radials. Performance of the radials is likely to be seriously overestimated when the uncertainty in the radial path and pressure losses in the radials are not taken into account.

1. INTRODUCTION

To economically produce a geothermal resource, wells with sufficient productivity are a key element. However, for a variety of reasons well productivity can be lower than expected or decline over time, for example because of disappointing reservoir transmissivity or because of well problems, such as scaling or near well bore damage. An option to enhance the productivity of a well is drilling small-diameter laterals. For bypassing a skin such a lateral need not be very long (up to 10 m should be enough), but for connecting the reservoir better to the well in case of e.g. low permeability, longer laterals are better. A technique which can achieve a distance of up to 100 m is Radial Jet Drilling (RJD) (see e.g. Kamel, 2017, Yan et al, 2018). This technique has been developed in the petroleum industry but is relatively new for geothermal applications and still under development. Laterals are jetted perpendicular to the well bore (backbone) using a hydraulic jet which is deflected in the well using a deflector shoe. One of the limitations of the jetting process, is that the jets cannot be steered and thus the realized path is uncertain. No observations of the path of jetted laterals in the subsurface exists in literature. The closest are the observations from jetting in a quarry described by Reinsch et al. (2018). These clearly showed that the lateral path is not straight.

The potential benefit of laterals (also called radials) has been analysed before. Peters et al. (2015, 2016) mainly used analytical tools to investigate the performance of RJD for Dutch geothermal applications. They concluded that the increase in productivity or injectivity due to radial stimulation of a single well in a homogenous reservoir depends almost linearly on the total length of the jetted laterals. Reservoir parameters which affect the increase most are the anisotropy in the permeability and the thickness of the reservoir. For homogeneous, tight gas fields, simulation results showed that the benefit of RJD stimulation was highest for low permeability reservoirs (Peters, 2015), which was determined by the limited gas volume that can be produced. For higher permeability, the available gas volume can more easily be produced without laterals within the given time frame. The uncertainty in the radial path was investigated in terms of length, inclination and diameter of the radials. Of these, length had most impact. Nair et al. (2017) included a more complete uncertainty analysis in an evaluation of the RJD job on the Klaipėda geothermal site in Lithuania and concluded that the uncertainty reduced the expected benefits considerably. The decrease in expected benefits was partially the result of heterogeneity of the reservoir, which was highly layered.

In this paper, we will investigate numerically the potential benefit of laterals in geothermal reservoirs including the impact of the uncertainty in the lateral path and reservoir heterogeneity. Two realistic case studies are simulated: a layered, sedimentary case and a dual porosity reservoir. The sedimentary site is based

on the Klaipėda geothermal site. The dual porosity site is based on the Californië geothermal site in The Netherlands. For these cases, a sensitivity analysis is performed to analyse the improvement in productivity/injectivity of the existing wells for different numbers of laterals with uncertain lateral path.

2. CASE 1: KLAIPĖDA

2.1 Model description

The Klaipėda geothermal plant is located within the West Lithuanian geothermal anomaly with a relatively high heat flow density of 70-90 mW/m^2. The reservoir is composed of a fine-grained friable sandstone (fine and medium grained) from the Lower Devonian called the Kemeri formation (Šliaupa, 2016). The reservoir has relatively thin reservoirs layers with high permeability between thicker layers of fine-grained material with low permeability. In total four wells were drilled: two injectors and two producers (Brehme et al, 2018). To simplify the simulations and interpretation of the results only two wells were used in this model: 1I and 2P.

Three facies are identified: coarse sand, fine sand and clay. Permeability and porosity are constant per facies (Table 1), because it is assumed that the variability between the facies is much larger than the variability within a facies. The vertical distribution of the facies is modelled based on the gamma ray log in both wells and upscaled the fine, geological grid (20 m x 20 m x 1.3 m). Facies distribution was simulated on this fine grid using sequential indicator simulation based on the upscaled facies logs in the wells. The constant permeability and porosity per facies were implemented in the fine grid and subsequently upscaled to the coarser simulation grid. Flow-based upscaling with harmonic averaging was used for upscaling the permeability (Schlumberger, 2017). Further settings and input of the model can be found in Table 1. The reason for choosing sequential indicator simulation rather than kriging for generating the facies distribution, is that the goal of this model is not the best representation of this reservoir, but creating a reservoir with realistic heterogeneity. In Figure 1 (see end of this section), a cross section is presented which shows the permeability in the coarse simulation grid and the two wells.

The model is not history matched to observed data, although a check was done to verify that the productivity of the wells was within the range observed. The wells have many issues with decreasing productivity/injectivity over time, in particular the injector (Brehme et al., 2017). This has not been included in this study. Both wells 1I and 2P are vertical and are run on a rate constraint of 9600 sm^3/d. Viscous pressure drop in the laterals is not included in the simulations.

Table 1: Input for the Klaipėda model

Grid	
Grid Cells (Ni x Nj x Nk)	92 x 114 x 34
dx x dy x dz	50 m x 50 m x 4.5 m
Depth interval	915 to 1130 m TVDSS
Rock properties (fine grid)	
k_h (Coarse sand, fine sand, clay)	1400 mD, 300 mD, 0.005 mD
Porosity (Coarse sand, fine sand, clay)	0.26, 0.18, 0.05
Rock compressibility	0.00009 bar^{-1}
Kv (case 1, case 2)	kh /10 (case 1) and kh /2 (case 2)
Net/Gross	1
Thermal properties	
Thermal conductivity (sand, clay)	194 kJ/m/d/K, 161 KJ/m/d/K
Specific heat capacity (rock, fluid)	2300 kJ/m^3/K, 3.9 kJ/kg/K
Initial Reservoir Conditions	
Pressure	107.2 bar @ -1047.5 m
Temperature	39° C @ 1050 m
Thermal gradient in the reservoir	2 °C / 100 m
Water Properties	
Density @ ref. conditions	1055.4 kg/m^3
Viscosity (@ 10, 38, 80 °C)	1.4, 0.88, 051 cP
Formation Volume Factor	1.0004 rm^3/sm^3
Compressibility	0.000037 bar-^{1}
Salinity	95 g/l

2.2 Scenarios

Although in reality only well 1I was stimulated with RJD with laterals of length up to 40 m, in this case both wells of the doublet (1I and 2P) will be stimulated and the maximum length is 100 m. Three stimulation scenarios were run: one with 4 laterals, one with 8 laterals and one with 12. The radials are distributed over 4 kick-offs in both wells for the 12-radial case (Figure 2). For the cases with fewer radials, kick-offs are removed. For the 8-radial case, the middle kick-off is removed for both 1I and 2P. For the 4 radial case, only the top kick-off is selected.

All three radial scenarios are run with two cases for the vertical permeability k_v (before upscaling): $k_v = k_h/10$ (case 1) and $k_v = k_h/2$ (case 2) (Table 1).

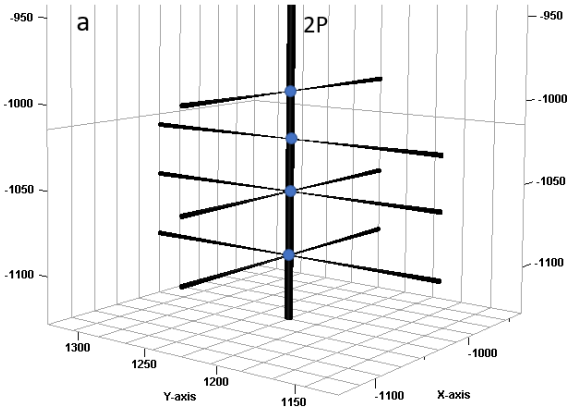

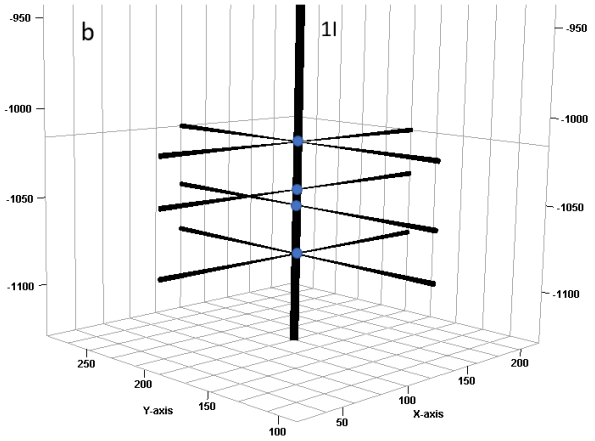

Figure 2. Radial well configuration of well 2P (a) and 1I (b) for the 12-radial case. Blue dots indicate kick-off points.

To account for uncertainty in the radial path, the radial paths were varied. 30 Realizations of the radial paths were made and the resulting flow simulated. The realizations were created by sampling from uniform uncertainty ranges for kickoff depth, length, azimuth inclination and diameter of the laterals. Sampling was done according to a Latin Hypercube scheme. The uncertainty ranges are presented in Table 2. Absolute ranges mean that the values used in the simulation are sampled from that range. Relative ranges mean that the values sampled from the range are added to the base value, e.g. for the kick-off depth. The minimum value for the length is quite small, because of concerns about the stability of the laterals in the friable Kemeri Formation. The range of the radial diameter is quite large, because this includes potential effects of skin and viscous pressure drop due to flow in the lateral. Nair et al (2017) showed that the impact of diameter on the inflow is relatively small. Viscous pressure drop can be important for high flow rates and because of the very irregular and rough inner diameter of a lateral compared to normal tubing. Inclination is defined as an absolute range assuming a horizontal base position of the radial.

The representation of the uncertainty in the lateral path is quite simplified here. The laterals are always assumed to be straight and uniform along their entire length. However, representation of these details is beyond the scope of this study and probably has a smaller effect than the factors included here.

Table 2. Uncertainty quantification for the radials.

	Type of uncertainty	Minimum value of the range	Maximum value of the range
Length (m)	absolute	10	100
Diameter (m)	absolute	0.001	0.1
Inclination (°)	absolute	45*	135*
Azimuth (°)	relative	-90	90
Kickoff (m)	relative	-2	2

* 90 ° is horizontal.

In this analysis we have chosen to analyse the productivity and injectivity of both wells after 10 years for all cases. The reason is that in particular the injectivity declines because of the lower viscosity of the injected, cold water. As the cold water area expands, injectivity declines. This is illustrated in the Figure 3 below for the case without radials.

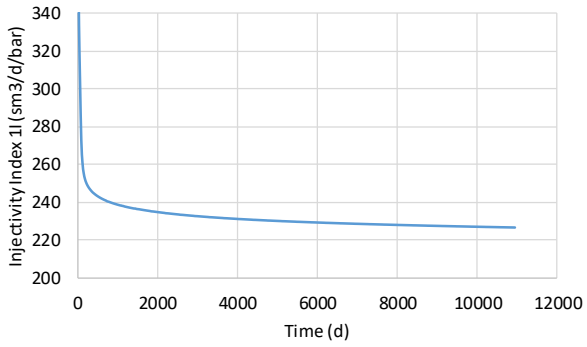

Figure 3. Development of the transient injectivity index of well 1I (sm^3/d/bar) over time.

2.3 Results

The average increase (from the 30 realizations) as a result of stimulation with 4, 8 or 12 radials is presented in Table 3. The productivity index (PI) for well 2P is always higher. This is expected, because the permeability encountered in this well is larger. However, also the increase resulting from radials is larger (Table 3). In analytical modelling studies (Peters et al., 2015; Peters et al., 2016), it was shown that the permeability does not impact the relative increase due to radials. The reason for the larger increase due to radial stimulation is probably due to the larger vertical permeability after upscaling in the area of well 2P. Both the horizontal and vertical permeability as listed in Table 1 have been applied in the fine grid and subsequently upscaled. This means that the effective ratio horizontal over vertical permeability in the coarser simulation grid can be quite different.

The increase in vertical permeability shows hardly any effect for well 1I in case of 4 radials (20.0% versus 23.2%). This is due to the upscaling of the vertical permeability. In the area of the radial kick-off in the 4-radial case, upscaled vertical permeability is very small due to the large number of clay layers.

Table 3. Increase in well productivity/injectivity due to radial stimulation (in %) (average of 30 realizations).

	1I		2P	
	k_v = 0.1*k_h	k_v = 0.5*k_h	k_v = 0.1*k_h	k_v = 0.5*k_h
4 radials	20.0	23.2	29.5	31.5
8 radials	46.9	60.2	59.4	68.0
12 radials	66.5	78.4	71.9	83.3

The increase from adding extra radials is not the same going from 4 to 8 and from 8 to 12. This is mostly determined by the local permeability in the vicinity if the radials. However, because the increase in injectivity/productivity is calculated for the operating

doublet, the wells influence each other. For example, if injectivity improves, the increase in pressure around the well is less, which has a negative impact on the productivity of the producer. For the behaviour of a single well, it is better to analyse the well only. However, in a real case, wells are run in a doublet setup and therefore this analysis is considered relevant for field applications.

It should be noted that although a sample size of 30 realizations was used, still some difference occurs for different samples. This is however not more than a few percent.

In Figures 4 and 5 the results for all simulations are presented in the form of Box-Whisker plots of the productivity Index (PI) /Injectivity Index (II), which also shows the range of the results of the 30 simulations. The uncertainty range is smaller for well 1I and smaller for 4 radials than for 8 or 12 radials. The uncertainty ranges overlap for the 8 and 12 radial cases. The discrepancy with the expected increase without including uncertainty is considerable: for example for $k_v = 0.1*k_h$ for 12 perfect radials the expected increase is 474 and 822 sm^3/day/bar for 1I and 2P respectively. From Figure 4, it is clear that this is well outside the expected range when including uncertainty. The same is true all the other cases.

The impact of the radials on the breakthrough of cold water was also evaluated. A decrease in temperature of the produced water is simulated after approximately 30 years. When averaged over the 30 realizations, the impact of the radials is minimal (< 0.1 °C). The spread between individual realizations is a bit larger, but generally below one degree at any given time. Since the rate is kept constant for all simulations, this is expected.

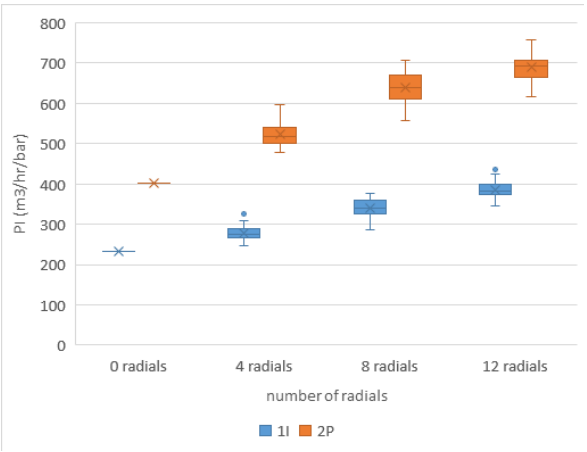

Figure 4. Box-Whisker plots of PI / II for producer 2P and injector 1I for kv/kh = 0.1 (The boxes indicate the quartiles, the lines extending vertically indicate the minimum and maximum (the 'whiskers'), the average is given by a cross and outliers are indicated as dots.)

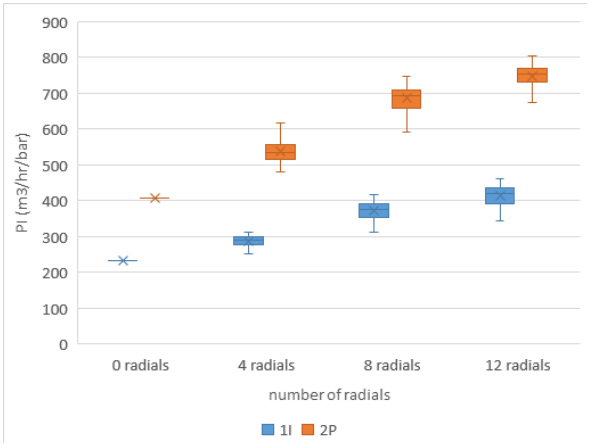

Figure 5. Box-Whisker plots of PI / II for producer 2P and injector 1I for kv/kh = 0.5. Explanation see Figure 4.

In these simulations, viscous pressure drop inside the well and the radials was not included. This means that the results are independent of the rate. However, Peters (2015) showed that in case of gas flow through laterals with small diameter (< 0.05 m), pressure drop can be significant. Therefore, the impact of viscous pressure drop on the injectivity index resulting from radial stimulation was evaluated. This was done by including viscous pressure drop calculations in the reservoir simulations. Viscous pressure drop is calculated using the Darcy-Weissbach equation:

$$dP = 2f\frac{L\rho v^2}{D} \qquad [1]$$

Where:

f : Fanning friction factor
D : tubing inner diameter
ρ : fluid density
v : fluid velocity
L : length of the tube (in this case, radial)

The Fanning friction factor is determined according to Haaland (1983), which is valid for turbulent flow. The friction factor depends on the absolute roughness, which can be interpreted as the distance between the peaks and throughs on the surface of the tubing/radial. The absolute roughness was taken quite large at 0.01 m, because the inner surface of the jetted radials is expected to be much rougher than normal tubing.

The impact was evaluated for a single, vertical well with 4 radials in a homogenous reservoir for a rates up to 7200 m^3/d. Injectivity of the well is similar to well 1I. The radials are 100 m long and have a diameter of 0.05 cm. In this case, uncertainty of the radial path is not included. In Figure 6 and Figure 7 the results are presented. Without pressure drop, the injectivity of the well is independent of the rate and is 322 m^3/d/bar, which is an increase of 57% compared to the well without radials. When pressure drop is accounted for, the increase due to stimulation (Figure 6) is only 32 % for a rate of 7200 m^3/d. This impact is considerable and means that for high rate wells, more radials are required.

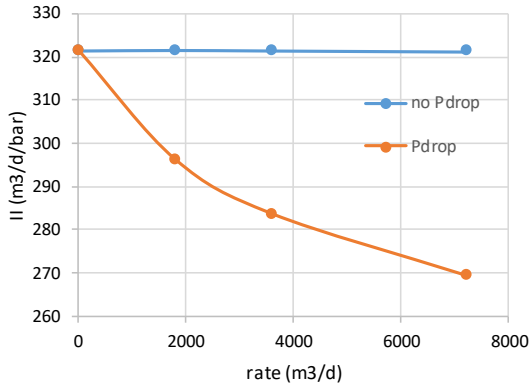

Figure 6. Injectivity Index (II) as a function of rate when pressure drop is included.

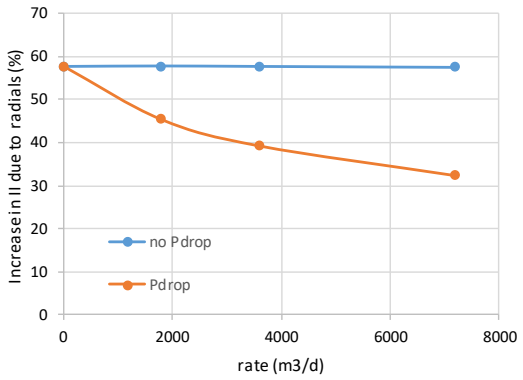

Figure 7. Increase in Injectivity Index (II) due to stimulation with radials as a function of rate when pressure drop is included.

This case study shows that generic analysis of improvement resulting from radial stimulation is challenging, due to the variability that can be expected in real cases. Local permeability has a large impact on the actual performance of the laterals.

Even if the permeability in the well has been observed, uncertainty is large because the radials move outside of the near-well area. Including the effects of uncertainty in the radial path and for high rates the viscous pressure drop is necessary to achieve realistic predictions of the benefits of radial jetting.

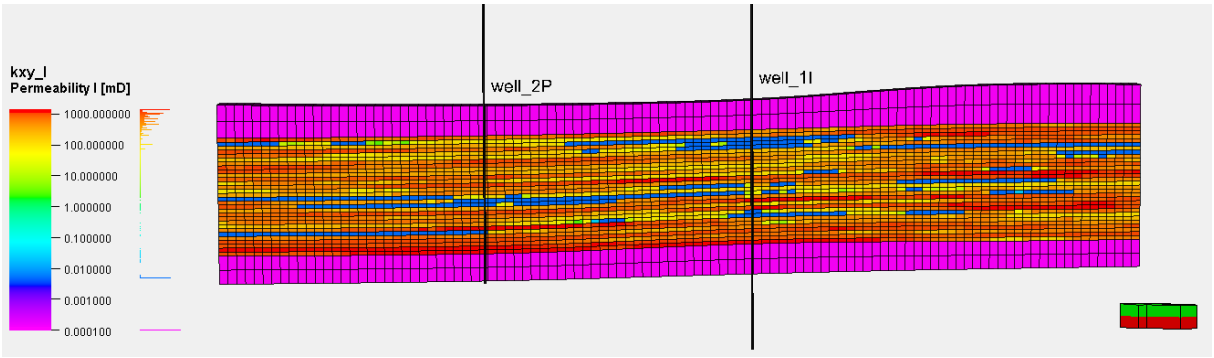

Figure 1: Vertical cross-section of the reservoir model showing the horizontal permeability (vertical exaggeration is 5; length = 5700 m).

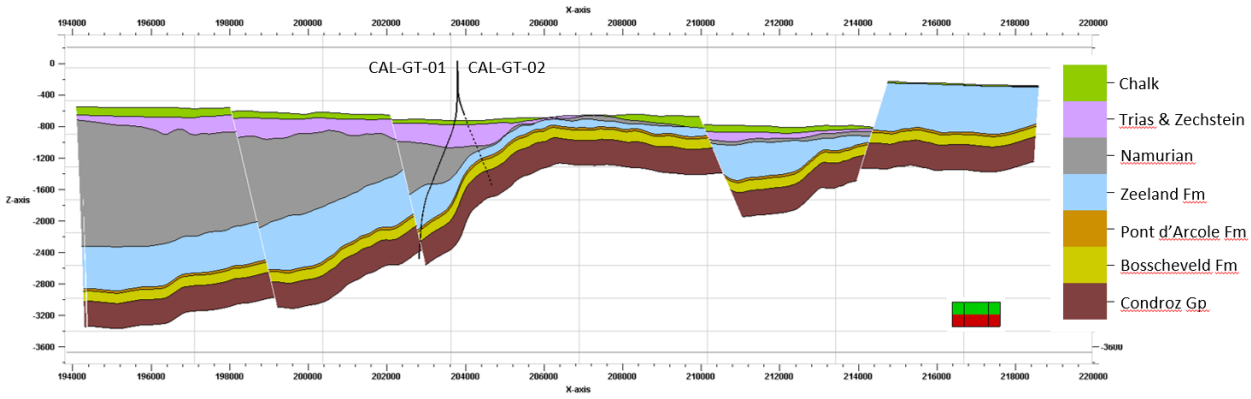

Figure 8. Cross section of the Californië area.

2. CASE 2: CALIFORNIË

3.1 Model description

The Californië geothermal area is located near Venlo in the Netherlands. The area contains five geothermal wells: CAL-GT-01 through CAL-GT-05. In this case study, only wells CAL-GT-01 and CAL-GT-02, which are in the public domain are used. The wells have been planned as a doublet, but are currently not in operation. The producer CAL-GT-01 has good productivity and

the injector CAL-GT-02 has poor injectivity. The reason for this difference is that the producer is drilled in the direction of a major fault which has a productive fault zone. The injector is drilled away from the fault in an area with much lower permeability. The reservoir section of the wells comprises rocks belonging to four formations (Table 4 and Figure 8). Since the Californië boreholes penetrated a relatively unknown stratigraphic interval in The Netherlands, it was decided to follow the Belgian nomenclature for the lowermost three stratigraphic units, viz. The Pont d'Arcole Fm, the Bosscheveld Fm, and the Condroz Group.

In the well CAL-GT-01 production stems primarily from limestones belonging to the Zeeland Formation of Early Carboniferous (Dinantian) age. In well CAL-GT-02, the Zeeland Fm is much thinner (~80 m). It is assumed that the flow is distributed over the entire drilled depth, which includes the Devonian rocks of the Bosscheveld Formation and Condroz Group (Table 4). All formations have a tight matrix and are dominated by fracture flow. Therefore the area is simulated as a dual porosity medium.

Table 4 Reservoir section formations in Californië area

Name	Main lithology	Age
Zeeland Fm	limestone	Early Carboniferous (Visean)
Pont d'Arcole Fm	shale	Early Carboniferous (Tournaisian)
Bosscheveld Fm	Dolomites, shales, siltstones, sandstones	Late Devonian to Early Carboniferous (Famennian to Tournacian)
Condroz Group	sandstone/quartzite	Late Devonian (Famennian)

The thin Pont d'Arcole Formation (Table 4) separates the Zeeland Fm from the older siliciclastic rocks. It has not yet officially been described in the Dutch stratigraphy, but is known from Belgium and Germany. It does not contribute to production. Similarly, rocks belonging to the Condroz Group have not been described in the Dutch stratigraphy, but they are known from the Belgian stratigraphy. Rocks of Devonian age have seldomly been drilled in the Netherlands. In Belgium, on the other hand, Devonian rocks are mined at various opencast sites. A transition zone exists between these rocks and the dolomites and limestones of the Zeeland Formation. This zone contains rocks of varying lithological composition that are grouped into the informal Bosscheveld Formation. Rocks of this formation are claystones, limestones and sandstones.

A geological model has been created in-house by TNO, and is very similar to the model described in Reith (2018). Because of the complexity of the local geology and the limited availability of seismic data, the model uncertainty is quite high. The goal of the model is not a representation of the local situation, but a realistic dual-permeability model with variability in the fracture density. Therefore, the model is not history matched to actual production data.

The main control on the fracture distribution is assumed to be the faults. Around faults, often a damage zone occurs which has increased permeability (e.g. Johri et al. 2013; Bauer et al., 2016) due to fractures. The width of this zone depends amongst others on the history of the fault (especially displacement) and the rock type. Hydrothermal alteration can further impact the permeability of the fractures. It is not known how wide the fault damage zone around the Tegelen fault is. However, from the high injectivity of CAL-GT-01, it is likely that such a zone exists. For the model, it is assumed that the fracture density depends on the distance to faults (d) and can be calculated as:

$$I_{fr} = 0.5d^{-0.8} + 0.5e^{-d^2/(2*220*220)} \quad [2]$$

To account for the orientation of the fractures the fracture permeability k_{fr} is taken anisotropic: the horizontal (along bedding) permeability perpendicular to the fault (j-direction) is taken smaller than the permeability parallel to the fault (i-direction). The vertical (cross-bedding) permeability is taken as 10 % of the maximum horizontal permeability. In summary:

$$k_{fr,i} = 20I_{fr} \quad [3]$$

$$k_{fr,j} = 2000I_{fr} \quad [4]$$

$$k_{fr,k} = 200I_{fr} \quad [5]$$

Also the fracture porosity and matrix-fracture interaction have been made dependent on the fracture density (Table 5). Further input properties are listed in Table 5. The Pont d'Arcole Fm is assumed to have zero porosity and permeability.

The wells have a deviation of 35° at reservoir level and are both completed open hole with diameter of 0.22 m. They are run on rate constraint at the relatively modest rate of 2000 sm^3/d, because the injectivity of CAL-GT-02 is too poor to sustain higher rates.

Table 5. Overview of the Californië model properties.

Grid	
Grid Cells (Ni x Nj x Nk)	185 x 262 x 41
dx x dy x dz	50 m x 50 m x variable (mostly 10-20 m)
Depth interval	1500 to 2500 m TVDSS
Rock properties	
k matrix	10 mD (Zeeland Fm); 0.1 mD (Devonian)
Porosity matrix	0.04 (Zeeland Fm); 0.01 (Devonian)
k fractures	Depends on fracture density (see eq. 2 to 5)
Porosity fractures	$0.05*I_{fr}$
σ_v matrix/fracture coupling	$12*I_{fr}$

Rock compressibility	0.00001 bar^{-1}
Net/Gross	1
Thermal properties	
Thermal conductivity	224 KJ/m/day/K
Specific heat capacity (rock, fluid)	2700 kJ/m^3/K, 3.7 kJ/kg/K
Initial Reservoir Conditions	
Pressure	105 bar @ 1000 m
Temperature	62.5° C @ 1530 m
Thermal gradient	3.4 °C / 100 m
Water Properties	
Density @ ref. conditions	1034 kg/m3
Viscosity (@ 10, 50, 90 °C)	1.34, 0.67, 0.41 cP
Formation Volume Factor	1.017 rm^3/sm^3
Compressibility	0.00004 bar^{-1}
Salinity	50 g/l

3.2 Scenarios

Radials are only placed in well CAL-GT-02, because well CAL-GT-01 already has high productivity. Three scenarios for the radial well design were run: with 8, 12 and 16 radials. The radials are always grouped 4 per kick-off. The kick-offs are distributed over the length of the open hole part, which is 419.2 m. For the case with 12 radials, the kick-offs are shown in Figure 9 and are 30, 193 and 343 m AH below the casing shoe. For the 8 radial case, the top kick-off point is left out. For the 16 lateral case the kick-off depths are 30, 170, 270 and 370 m AH below the casing shoe. For the permeability, two scenarios were run in order to examine the impact of anisotropy: $k_i = 20I_{fr}$ (as described in the input) and $k_i = 200I_{fr}$ (10 times larger).

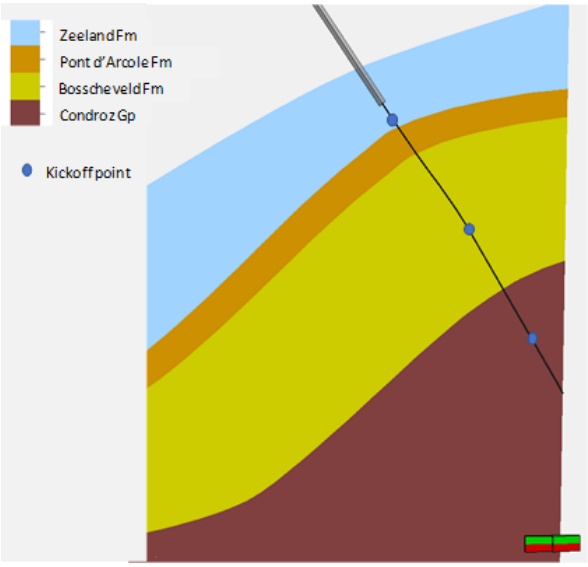

Figure 9. Cross section along well CAL-GT-02 showing the three kickoff points for the 12-radial case.

The uncertainty quantification is done in the same way as for the Klaipėda case, with the same settings for the uncertainty.

3.3 Results

An overview of the results is presented in Table 6, which shows the increase in injectivity of CAL-GT-02. The injectivity of the well was 11.9 sm^3/d/bar without stimulation for $k_{fr,i} = 20I_{fr}$ and 24.1 sm^3/d/bar for $k_{fr,i} = 200I_{fr}$. The increase in injectivity for this well is much larger than the increase achieved for Klaipėda, also for the same number of laterals. The reason for this is that the inflow into the radials in Klaipėda was dominated by the lower horizontal permeability, whereas the inflow into the vertical backbone was dominated by the higher horizontal permeability. For CAL-GT-02, both the backbone and the radials are dominated by all three permeabilities, although the backbone benefits more from the increased i-direction permeability than the laterals: the increase for the scenario with $k_{fr,i} = 200I_{fr}$ is less than for $k_{fr,i} = 20I_{fr}$.

The impact of the radials on the produced water temperature was examined. Cold water breakthrough doesn't occur in this doublet within 50 years, because of the favourable orientation of the fracture permeability which diverts the cold water away from the production well. The production water temperature is influenced by the placement of the radials: deeper radials increase the pressure in deeper layers and thus increase the temperature of the produced water.

Table 6 Increase in well injectivity for CAL-GT-01 due to radial stimulation (in %) (average of 30 runs).

	$k_i = 20I_{fr}$	$k_i = 200I_{fr}$
8 radials	68.2	43.5
12 radials	126.3	77.2
16 radials	162.0	98.5

In Figures 10 and 11 the injectivity index II is presented for all scenarios. The uncertainty ranges from the cases with 8 and 12 radials are similar to Klaipėda. For the 16-radial case the uncertainty range becomes larger and shows much overlap with 12-radial case. Just as for the Klaipėda case, the increase in productivity calculated for perfect radials without uncertainty is much larger: for example for $k_i = 20I_{fr}$ and 12 radials the simulated injectivity is 47 sm^3/d/bar which is higher even than the maximum for 16 radials.

It should be noted that due to the coarseness of the grid, the numerical error of the simulation of the radials is probably quite large (Peters et al., 2018). However, this is not likely to change the overall results.

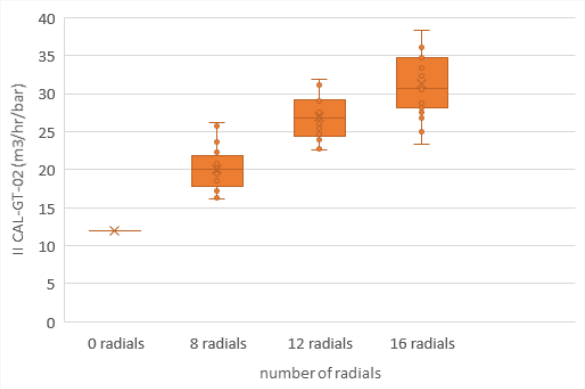

Figure 10. Box-Whisker plots of the injectivity index (II) for CAL-GT-02 for $k_{fr,i} = 20I_{fr}$. Explanation see Figure 4. Dots represent all values.

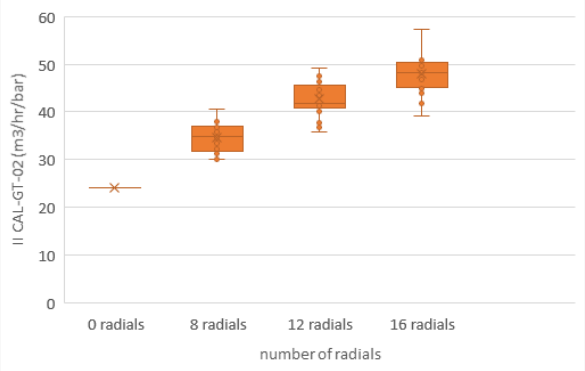

Figure 11. Box-Whisker plots of the injectivity index (II) for CAL-GT-02 for $k_{fr,i} = 200I_{fr}$. Explanation see Figure 4. Dots represent all values.

3. DISCUSSION AND CONCLUSIONS

The results presented above and in particular the ranges in injectivity/productivity depend heavily on the uncertainty ranges as listed in Table 2. Preferably these uncertainty ranges should be adjusted to the local conditions. However, information about the impact of local subsurface conditions such as in-situ stress and fractures on the uncertainty is currently insufficient. From experimental work of jetting under true-triaxial conditions (Bakker et al., in prep.), it appears that jetting in the direction of minimum principal stress is easier than in the direction of maximum principal stress. This could mean that radials tend to get oriented in the direction of the least principal stress. In the experiments, a deviation in the direction of jetting was not observed, but this could be due to the shortness of the jetted path (~20 cm). In the jetting experiments in the quarry (Reinsch et al., 2018), the laterals did seem to be oriented in one direction (upwards), however no clear reason could be identified for this. For the Californië area, which is in a normal faulting regime, the laterals would in that case be oriented perpendicular to the faults. However, testing of jetting through fractures (Bakker et al., in prep.), showed a clear decrease in speed when jetting through a fracture. For larger fractures, the jetting is likely to be halted. This would indicate that laterals parallel to the fault are likely to be more successful. At this point in time, it is not clear how these conflicting effects will work out in practice. Therefore, in both case studies the same uncertainty ranges were used.

From the cases studied in this paper, it is clear that the potential for radial stimulation is good: in all scenarios significant increase in the injectivity or productivity was achieved. However, predictions of expected increase due to radials are inherently highly uncertain because of the uncertainty in the radial path and because of the dependence on the detailed permeability distribution around the well. In general, systems in which the main well is not optimally oriented with respect to the main permeability direction are beneficial for radial stimulation. The radials can take advantage of the higher permeability, assuming that they are stable. In general in thicker reservoirs or reservoirs with high flow rates, more radials are required. For wells with high flow rate, more radials are required to keep frictional pressure drop in the radials down. The results shown here confirm the conclusion by Nair et al (2017) that not taking into account the uncertainty in the radial path results in overestimation of the expected increase in production.

REFERENCES

Bakker, R. R., Hahn, S., Friebel, M., Bruhn, D. F. , Reinsch, T, and Barnhoorn, A.: A laboratory study on radial jet drilling in true triaxial stress conditions. In preparation.

Bauer, H., Schröckenfuchs, T. C. and Decker, K.: Hydrogeological properties of fault zones in a karstified carbonate aquifer (Northern Calcareous Alps, Austria). *Hydrogeol J* , **24**, (2016) 1147–1170. DOI 10.1007/s10040-016-1388-9.

Brehme, M., Blöcher, G., Regenspurg, S., Milsch, H., Petrauskas, S., Valickas, R., Wolfgramm, M. and Huenges, E.: Approach to develop a soft stimulation concept to overcome formation damage – A case study at Klaipeda, Lithuania. PROCEEDINGS, 42nd Workshop on Geothermal Reservoir Engineering, Stanford University, Stanford, California (2017).

Brehme, M., Regenspurg, S., Leary, P. et al., "Injection-Triggered Occlusion of Flow Pathways in Geothermal Operations," Geofluids, vol. 2018, Article ID 4694829, 14 p (2018). https://doi.org/10.1155/2018/4694829.

Haaland, S.E. Simple and explicit formulas for the friction factor in turbulent pipe flow, Transactions of the ASME, *Journal of Fluids Engineering* (1983) 105, No. 1, 89-90.

Johri, M., Zoback, M., Dunham, E.M. and Hennings, P.: Fault Damage Zones-Observations, Dynamic Rupture Modeling and Implications on Fluid Flow. AAPG Search and Discovery Article #41249. (2013).

Kamel, A.H. 2017. A technical review of radial jet drilling. J. of Petroleum and Gas Eng. 8(8), (2017), 79-89. DOI: 10.5897/JPGE2017.0275

Nair, R. Peters, E., Šliaupa, S., Valickas, R., Petrauskas, S.: A case study of radial jetting technology for enhancing geothermal energy systems at Klaipėda geothermal demonstration plant. PROCEEDINGS, 42nd Workshop on Geothermal Reservoir Engineering, Stanford University, Stanford, California, (2017).

Peters, S.A. Production Performance of Radial Jet Drilled Laterals in Tight Gas Reservoirs in the Netherlands. A Simulation Approach and Economic Analysis. Delft, The Netherlands (2015). Msc Thesis TUDelft.

Peters, E., Veldkamp, J.G., Pluymaekers, M.P.D. and Wilschut, F.: Radial jet drilling for Dutch geothermal applications, *TNO*, Utrecht, (2015) R10799.http://publications.tno.nl/publication/34620510/4C8joC/TNO-2015-R10799.pdf

Peters, E., Blöcher, G., Salimzadeh, S., Egberts, P.J.P., and Cacace, M.: Modelling of multi-lateral well geometries for geothermal applications. *Adv. Geosci.* **45**, (2018) 209-215. https://doi.org/10.5194/adgeo-45-209-2018.

Peters, E., J.G. Veldkamp, M.P.D. Pluymaekers and F. Wilschut: Radial jet drilling for Dutch geothermal applications. EGC2016 Strasbourg, 19-24 Sept. Proceedings EGC. (2016).

Reinsch, T., Paap, B., Hahn, S., Wittig, V. and van den Berg, S.: Insights Into the Radial Water Jet Drilling Technology - Application in a Quarry. DOI: 10.1016/j.jrmge.2018.02.001. 2018.

Reith, D.F.H. 2018. Dynamic simulation of a geothermal reservoir. Case study of the Dinantian carbonates in the Californië geothermal wells, Limburg, NL. Msc thesis TUDelft (public version).

Schlumberger: Petrel® User Manual v2017.2. (2017)

Šliaupa, S.: Reservoir characterisation of the Klaipėda geothermal plant (Lithuania), Vilnius, Lithuania (2016). Nature Research Centre report.

Yan, J., Cui, M., He, A., Jiang, W. and Liang, C. Study and Application of Hydraulic Jet Radial Drilling in Carbonate Reservoirs. International Journal of Oil, Gas and Coal Engineering. Vol. 6, No. 5, (2018), pp. 96-101. DOI: 10.11648/j.ogce.20180605.13.

Acknowledgements

The research for this paper received funding from the European Union's Horizon 2020 research and innovation programme under grant agreement No. 654662 (SURE). The content of this paper reflects only the authors' view. The Innovation and Networks Executive Agency (INEA) is not responsible for any use that may be made of the information it contains. The use of data from the Klaipėda site received from Geoterma and from the Californië site from Pieter Wijnen (via NLOG.nl) is gratefully acknowledged. The use of open source codes Field-Opt by NTNU and OPM-flow (https://opm-project.org/) is gratefully acknowledged.